# Unguided Cracking in Unsaturated Soils through a Coupled Nonlocal Poromechanics Model

Shashank Menon<sup>1</sup> and Xiaoyu Song, Ph.D.<sup>2</sup>

### **ABSTRACT**

We present a computational nonlocal poromechanics framework for modeling unguided cracking in unsaturated soils. In this mathematical model, the initiation and propagation of cracks in unsaturated soils is autonomous and modeled through a novel fracture criterion considering solid-fluid coupling effects. The nonlocal coupled poromechanics model is implemented numerically using an implicit fractional step algorithm in which the coupled problem is transformed into two sub-problems (i.e., mechanical and fluid flow). First, the mechanical sub-problem is solved using Newton's method with an explicit predictor of water pressure. Second, the sub-problem of fluid flow is solved using Newton's method in the updated solid configuration. Two numerical examples are presented to demonstrate the robustness of this proposed computational nonlocal poromechanics framework for modeling arbitrary cracking in unsaturated soils.

## INTRODUCTION

Desiccation cracking is a commonly occurring phenomenon in the drying process of unsaturated soil (Fredlund and Rahardjo 1993). Decreasing moisture content causes an increase in matric suction and shrinkage of soil volume which, when prevented, leads to tensile cracking in the soil. As such, desiccation cracking is a coupled flow-deformation process that leads to evolving discontinuities in the domain. Consequently, desiccation cracking has a significant effect on the engineering properties of soils by effectively increasing permeability of the medium and decreasing the mechanical strength of the soil (Lu and Likos 2004). Thus, it represents a significant danger to the integrity of earthen retaining elements like dikes and embankments, the viability of liner material for landfills, irrigation potential of soils and more (Lu and Likos 2004). Due to the significance of the phenomenon to broad spectrum of scientific disciplines, desiccation cracking has attracted significant research interest. Numerical modeling of desiccation cracking has provided deep insight into the physics of crack initiation and propagation (see Menon and Song 2019 for an in-depth review). For example, the initial water saturation level, subsequent change during evaporation and the resulting volume change (characterized by the water-retention curve) are the mechanism behind cracking. However, due to difficulties associated with measuring and tracking soil shrinkage, crack growth and joining and fluid flow in a fractured medium it is advantageous to develop a fully coupled computational framework capable of modeling of unguided, three-dimensional crack propagation and joining.

Classical poromechanics, based on local interactions, uses partial differential equations to describe the coupled solid deformation and fluid flow system, which leads to singularities at

<sup>&</sup>lt;sup>1</sup>Doctoral Student, Engineering School of Sustainable Infrastructure and Environment, Univ. of Florida, Gainesville, FL. Email: smenon92@ufl.edu

<sup>&</sup>lt;sup>2</sup>Associate Professor, Engineering School of Sustainable Infrastructure and Environment, Univ. of Florida, Gainesville, FL (corresponding author). Email: xysong@ufl.edu

discontinuities in the problem domain. An alternative theory of continuum mechanics, peridynamics was developed to unify the modeling of solid mechanics, fracture, and long-range forces. The global balance laws are formulated in terms of spatially integral equations with the domain of integration defined by an explicit length scale. Since no spatial derivatives are required, the formulation admits discontinuities in the field variables without additional remedial techniques and the governing equations remain valid on and off cracks in the domain (Song and Khalili 2019, Song and Silling 2020). This capability of peridynamics has made it an attractive option in modeling discontinuous processes in a variety of materials. Though initially developed for metals, recently, peridynamics has been extended to the multiphysics analysis of failure (Song and Menon 2019, Menon and Song 2020, 2021a, 2021b) and fracture in unsaturated porous media (Menon and Song 2019) via periporomechanics. In this study, the recently proposed periporomechanics (e.g., Menon and Song 2021a, 2021b) is extended for modeling unguided cracking in unsaturated porous media. We conduct numerical simulations of crack propagation in the two-dimensional and three-dimensional cases to demonstrate the robustness of the proposed computational nonlocal poromechanics model.

### FORMULATION & IMPLEMENTATION

A summary of the proposed nonlocal poromechanics framework is provided in this section. A point on the notation used in this study: boldface represents a vector quantity; bold italics represent a tensor quantity and underscores are used to differentiate peridynamic state quantities from classical point associated quantities. Periporomechanics conceptualizes multi-phase geomaterials as a homogenized collection of mixed material points of finite volume that can interact with each other over a finite distance, termed the horizon  $\delta$ . The horizon is an explicitly defined length scale parameter, embedded in the global balance laws, that demarcates the neighborhood,  $H_x$ , of a material point  $\mathbf{x}$ . The interactions between material points are termed bonds and all material field variables are tracked by mathematical quantities termed 'states' which act along said bonds. Each material point has two types of degree of freedom, i.e., displacement and fluid pressure. As such, the formulation is the nonlocal equivalent of the classical u-p formulation (Zienkiewicz et al. 1999). Deformation and fluid flow are imposed along 'bonds' between two material points  $\mathbf{x}$  and  $\mathbf{x}'$ ,

$$\underline{X} = \xi = x' - x$$

where  $\underline{\mathbf{X}} = \boldsymbol{\xi}$  is the bond between a point and its neighbor and is the relative position vector from  $\mathbf{x}$  to  $\mathbf{x}'$ . For the solid skeleton, the fundamental kinematic quantity is the deformation vector state  $\underline{\mathbf{Y}}\langle\boldsymbol{\xi}\rangle$  associated with individual interactions between material points,

$$\underline{Y}\langle\xi\rangle=y'(x')-y(x)\quad\text{,}\quad y(x)=x+u\quad\text{,}\quad y'(x')=x'+u'$$

where  $\mathbf{y}$  and  $\mathbf{y}'$  are the positions of  $\mathbf{x}$  and  $\mathbf{x}'$  in the deformed configuration,  $\mathbf{u}$  and  $\mathbf{u}'$  are the displacements at material points  $\mathbf{x}$  and  $\mathbf{x}'$  and the  $\langle \cdot \rangle$  is the bond with which the deformation state is associated with. Similarly, for the fluid phase, the primary variable is the pressure potential scalar state which reads,

$$\underline{\Phi}\langle \boldsymbol{\xi} \rangle = p'(x') - p(x)$$

and is evidently the relative difference in water pressure along the bond. The deformation and pressure potential states represent a more general picture of the deformation and flow potential than the corresponding gradient operator of classical mechanics. That said, through the reduction operation (Song and Silling 2020) over the horizon, the deformation and pressure potential states can be used to determine a nonlocal approximation of the gradient operator. For the solid skeleton, the derived variable is the effective force vector state  $\underline{\tilde{T}}(\xi)$  which is obtained from the skeleton resistance to deformation and can be decomposed as (Song and Silling 2020)

$$\underline{\widetilde{\mathbf{T}}}[\mathbf{x}]\langle \boldsymbol{\xi} \rangle = \underline{\mathbf{T}}[\mathbf{x}]\langle \boldsymbol{\xi} \rangle + S_r \underline{\mathbf{T}}_w[\mathbf{x}]\langle \boldsymbol{\xi} \rangle$$

where,  $\underline{\mathbf{T}}$  is the total force state,  $S_r$  is the degree saturation of water and  $\underline{\mathbf{T}}_w$  is the apparent capillary force state related to the matric suction. The degree saturation is a function of  $p \leq 0$  via the van Genuchten soil water retention curve (Fredlund and Rahardjo 1993). It is worth noting that we assume tension is positive for deformation and pore pressure is positive in compression following continuum mechanics convention. Using the effective force principle, the balance of momentum in a three-phase periporomechanics mixture can be expressed as,

$$\int_{H_{x}} (\underline{\tilde{\mathbf{T}}} - S_{r} \underline{\mathbf{T}}_{\mathbf{w}}) - (\underline{\tilde{\mathbf{T}}'} - S_{r}' \underline{\mathbf{T}'}_{\mathbf{w}}) dV' + (\rho_{s}(1 - \phi) + S_{r} \phi \rho_{w})(\mathbf{g} - \ddot{\mathbf{u}}) = 0$$
 (1)

where we have dropped the explicit dependence on the location and bond for brevity and,  $\phi$  is the skeleton porosity,  $\rho_s$  is the intrinsic solid density,  $\rho_w$  is the intrinsic liquid density, g is the vector of gravity and  $\ddot{\mathbf{u}}$  is the skeleton acceleration. For the liquid phase, the derived variable is the fluid flow state  $\underline{\mathbf{Q}}[\mathbf{x}]\langle \xi \rangle$ . Under the standard poromechanics assumptions of an incompressible solid phase, a passive gas phase and a barotropic liquid phase, we can express the balance of mass of a periporomechanics mixture using a single equation as follows,

$$\frac{\mathrm{d}S_r}{\mathrm{d}t} + S_r \int_{H_{\lambda}} \left( \dot{V}_s - \dot{V}_s^{\dagger} \right) \, \mathrm{d}V^{\dagger} + \frac{1}{\rho_w} \int_{H_{\lambda}} \left( \underline{Q} - \underline{Q}^{\dagger} \right) \mathrm{d}V^{\dagger} + Q_s = 0 \tag{2}$$

where  $V_{x}$  and  $\dot{V}_{x}$  are the states representing rate of volume change at x and x',  $\underline{Q}$  and  $\underline{Q}_{x}$  are the fluid flow states at x and x' respectively, and  $Q_{x}$  is the sink term. The first integrand represents the coupling term, the volume change of the solid skeleton, and the second integrand the mass transport of the liquid in the pore space.

A defining feature of periporomechanics, is that unlike classical mechanics, the governing equations are valid both on and off discontinuities. Therefore, all that is required to model crack propagation in periporomechanics is a suitable criterion. In general, crack propagation is modeled through the feature of bond-breakage: interactions between a point and its neighbor are eliminated when some kinematic (stretch/rotations) or energy (strain/J-integral) based criteria is satisfied. The simplest and most popular criteria is the critical stretch criterion, where stretch is defined as

$$s = \frac{\underline{\mathbf{e}}}{|\boldsymbol{\xi}|} = \frac{|\underline{\mathbf{Y}}| - |\boldsymbol{\xi}|}{|\boldsymbol{\xi}|}$$

and bond breakage is implemented through the influence function such that,

$$\underline{\omega} = 0$$
,  $s \ge s_{cr}$ 

The influence function is a scalar state function that modulates the strength of the interaction between two points. In this study a uniform value of  $\underline{\omega}=1$  was chosen for all bonds. By setting the influence function to zero for a broken bond the effective force state of the bond is neglected when calculating the skeleton force at a point (but fluid force is still considered). This naturally leads to force redistribution to the remaining bonds in the horizon. This in turn may cause more bonds to exceed their critical stretch and cause them to fail as well, allowing a crack to grow autonomously and leading to progressive failure. Cracks in the domain are tracked through the scalar damage variable  $\zeta(\mathbf{x})$  which is defined as

$$\zeta(\mathbf{x}) = 1 - \frac{\int_{H_x} \underline{\omega} \, dV_{x'}}{\int_{H_x} \, dV_{x'}}$$

such that a value of '0' corresponds to a point with no bonds broken and '1' to a point with all bonds broken.

To close the system of equations in Eq. 1 and Eq. 2 constitutive models are required to relate the effective force state and fluid flow states to the deformation and pressure potential states, respectively. Constitutive models in the proposed framework can relate the force state in a bond to its own deformation only (the simplest formulation) or, more generally, to a weighted average of deformation in all bonds in the horizon. The former is termed a bond-based model and is a special case of the latter, which is termed state-based. State-based models have been applied to the modeling of localized failure in multiphase geomaterials, via a correspondence model (Menon and Song 2021a), and crack propagation via an ordinary model (Menon and Song 2019). For details on the specific models used and their implementation the reader is referred to the cited publications. When bond breakage occurs, the bond cannot carry mechanical loads but can still transmit the fluid force and facilitate mass transport. Now, to accurately model the physics of fracture propagation and its influence on the fluid motion in the fractured configuration, the physical models (effective force principle and Darcy's Law) need to be modified to account for the discontinuity in the deformed configuration. Once  $\zeta(\mathbf{x}) \geq \zeta_{fr}$  the material point is designated a fracture point. To compute the fracture flow at a fracture point, we relate the fracture permeability  $K_f$  to fracture width using the cubic law for one-dimensional flow (Lewis and Schrefler 1998),

$$K_f = \frac{a_f^2}{12}$$

where the fracture width is then calculated as follows,

$$a_f = \frac{1}{\mathcal{N}_{f,i}} \sum_{i=1}^{\mathcal{N}_{f,i}} \underline{\omega} \langle \boldsymbol{\xi}_{ij} \rangle [|\underline{\mathbf{Y}}_{ij}| \cos \psi_{ij} - |\mathbf{X}_{ij}|]$$

where *i* denotes the material point,  $\mathcal{N}_{f,i}$  is the number of neighbors whose bonds with point *i* have been broken, and  $\psi_{ij}$  is the angle subtended by the deformation and reference vector states of bond  $\xi_{ij}$ .

The formulated periporomechanics is solved via a Eulerian-Lagrangian meshfree spatial discretization scheme and a fractional-step implicit time integration scheme. Broadly, two classes of implicit time integration schemes can be considered to solve coupled fluid flow and solid deformation problems: the monolithic approach and the staggered approach (Lewis and Schrefler 1998). The monolithic or fully coupled solution scheme involves the solution of the coupled system at each Newton iteration of each time step. This can become time and resource intensive particularly, in scenarios involving greatly differing time scales (for example in reservoir geomechanics). Alternatively, the coupled problem can be solved in a staggered manner via a suitable operator split that decomposes the coupled system into independent subproblems to be solved sequentially. Such so-called fractional step algorithms employ some explicit relationship (a predictor) to separate the mechanical problem from the fluid flow problem. The solution to the first sub-problem is then used as an input to solve the subsequent sub-problem, resulting in an efficient solution procedure. However, staggered solution schemes are not always unconditionally stable even when the individual sub-problems are unconditionally stable. Therefore, care must be taken in the choice of operator split procedure used such that the component operators exhibit appropriate group characteristics (Lewis and Schrefler 1998). This ensures that the algorithm is unconditionally stable. In this study, we implement a fractional step algorithm (Zienkiewicz et al. 1999) wherein the mechanical sub-problem is solved first using an explicit predictor of water pressure. Subsequently, the converged displacement is used to solve the mass balance in the current, updated configuration. The explicit predictor for the pressure increment reads,

$$\Delta p_{n+1}^* = -\Delta t \left(\frac{1}{\chi}\right)_n \left\{ S_{r,n} \int_{H_\chi} \left(\dot{V}_{s,n+1} - \dot{V}'_{s,n+1}\right) dV' + \int_H \left(\underline{Q}_n - \underline{Q}'_n\right) dV' \right\}$$

where  $\chi_n = \varphi\left[\frac{\partial S_{r,n}}{\partial p}\right]$  is the storage coefficient, all fluid-related terms are calculated using the converged values of the previous load step (denoted by subscript 'n') and the volume coupling term is computed using current values (denoted by subscript 'n+1'). Using this predictor, the capillary force state can be approximated as follows,

$$\boldsymbol{\mathcal{P}}^{u}_{n+1} = \int_{H_{x}} \left[ S_{n+1}^{*} \underline{\mathbf{T}}_{w,n+1}^{*} - S_{n+1}^{\prime *} \underline{\mathbf{T}}_{w,n+1}^{\prime *} \right] dV^{\prime}$$

where both  $S_{n+1}^*$  and  $\underline{\mathbf{T}}_{w,n+1}^*$  are calculated using the predicted pressure. Then the balance of linear momentum can then be expressed as,

$$0 = \rho_{n+1}(\ddot{\mathbf{u}}_{n+1} - \mathbf{g}) - \int_{H_{\mathbf{v}}} \underline{\widetilde{\mathbf{T}}}_{n+1} - \underline{\widetilde{\mathbf{T}}}'_{n+1} dV' - \boldsymbol{\mathcal{P}}^{u}_{n+1}$$

where we note that the pressure force density acts as an external load on the skeleton through  $\mathcal{P}_{n+1}^u$ . Once the above equation has been solved for the displacement, we recalculate the volumetric deformation coupling term,

$$\mathcal{P}_{n+1}^{p} = \int_{H_{x}} (\dot{V}_{s,n+1} - \dot{V}'_{s,n+1}) \, dV'$$

which is used as an input to solve the balance of mass as follows,

$$0 = \chi_{n+1} p_{n+1} + \int_{H_r} \left( \underline{Q}_{n+1} - \underline{Q}'_{n+1} \right) dV' + S_{r,n+1} \mathcal{P}_{n+1}^p$$

# OBLIQUE CRACK PROPAGATION

In this example, we model the propagation of wing cracks due to tensile loading of a twodimensional specimen. Wing cracks grow at an angle from the edges of the shear fracture allowing the shear fracture to propagate by the coalescing of these tensile fractures. The specimen geometry and details of the pre-crack are provided in Figure 1. The zero-thickness precrack is inserted by selectively preventing bonds that intersect it from being formed.

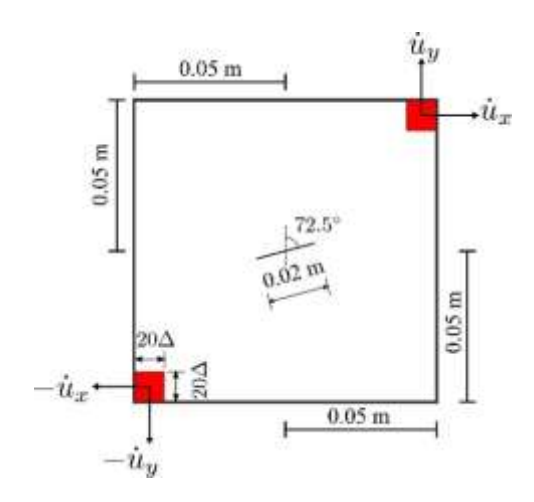


Figure 1. Schematic depicting the problem dimensions, crack geometry and location.

The problem domain is discretized using 20,000 mixed material points with  $\Delta = 1 \times 10^{-3}$  m. The material parameters are chosen as follows: solid density  $\rho_s = 2000$  kg/m³, bulk modulus  $K = 70 \times 10^4$  kPa, shear modulus  $\mu = 15 \times 10^4$  kPa, initial porosity  $\phi = 0.33$   $\rho_w = 1000$  kg/m³, saturated conductivity  $k_w = 1 \times 10^{-8}$  m/s, porosity index n = 1.785 and air-entry value  $s_a = 500$  kPa. The horizon is set to 3.05 $\Delta$ . The soil specimen has an initial matric suction s = 50 kPa, ( $S_r = 0.99$ ) and an initial isotropic stress state  $p'_0 = -50$  kPa.

The regions marked in red in Figure 1 represent the loading location. The displacement load is  $\dot{u}_x = \dot{u}_y = 10$  nm/s. No other skeleton boundary conditions are applied. For the fluid phase all boundaries are treated as impermeable. The simulation duration is t = 3000 s and time increment  $\Delta t = 0.5$  s.

Figure 2 plots the evolution of the resultant reaction force over applied displacement along the diagonal. The corresponding values of the applied displacement are  $u_x = u_y = (a) 2.1 \times 10^{-2}$  mm, (b)  $2.5 \times 10^{-2}$  mm and (c)  $2.7 \times 10^{-2}$  mm. Figure 3 and Figure 4 depict the scalar damage and water pressure in the problem domain at the aforementioned load steps, respectively.

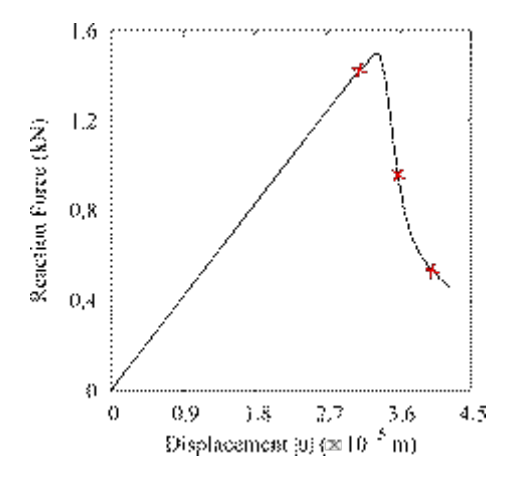


Figure 2. Reaction force over resultant displacement.

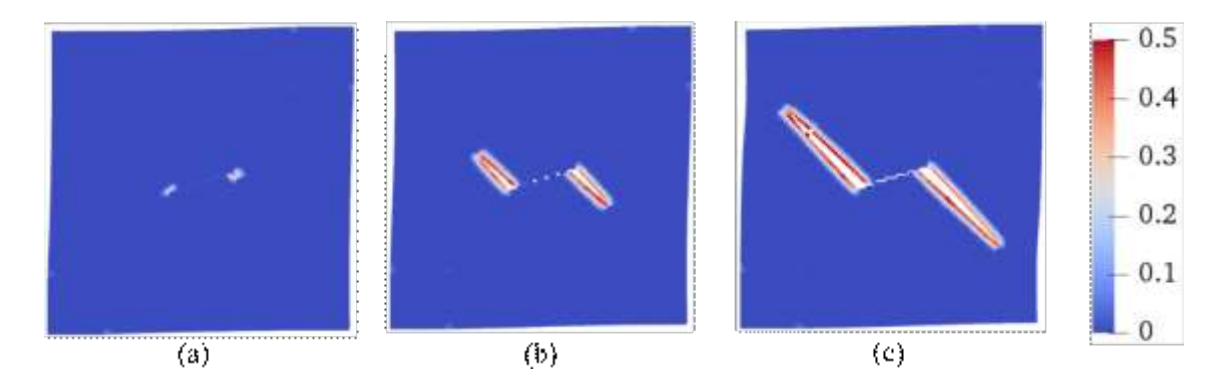


Figure 3. Contours depicting evolution of scalar damage at  $u_x = u_y = (a) 2.1 \times 10^{-2} \text{ mm}$ , (b)  $2.5 \times 10^{-2} \text{ mm}$  and (c)  $2.7 \times 10^{-2} \text{ mm}$ .

It is apparent that the crack opens parallel to the diagonal opposite to the loading direction. A scalar damage of 0.5 corresponds to interactions from one-half of the neighborhood being terminated. As the crack opens and propagates through the domain, a corresponding sharp discontinuity is visible in the pressure contour along the crack interface.

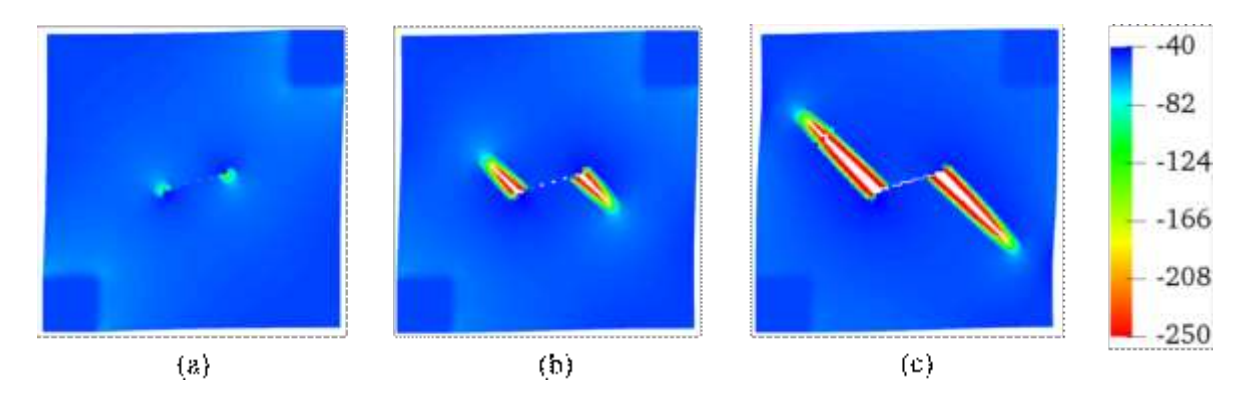


Figure 4. Contours depicting evolution of water pressure (in kPa) at  $u_x = u_y = (a) 2.1 \times 10^{-2}$  mm, (b) 2.5 x 10<sup>-2</sup> mm and (c) 2.7 x 10<sup>-2</sup> mm.

The crack changes the fluid flow in its vicinity acting as a preferential path for flow leading to the notable increase in matric suction (decrease in water pressure) in its immediate vicinity.

## LINEARLY RESTRAINED SOIL BAR

The ability of the proposed nonlocal poromechanics to predict soil cracking is further investigated in this section by simulating a linearly restrained, shrinkage induced soil cracking experiment. The soil sample was prepared and compacted in a long rectangular mold (300 mm long, 30 mm width and 12 mm height) as shown in Figure 5. The problem domain is discretized into 22,500 mixed material points with  $\Delta = 2 \times 10^{-3}$ m. The material parameters chosen are  $\rho_s = 2000 \text{ kg/m}^3$ ,  $K = 2.2 \times 10^3 \text{ kPa}$ ,  $\mu = 1.67 \times 10^3 \text{ kPa}$ ,  $\phi = 0.25$ ,  $\rho_w = 1000 \text{ kg/m}^3$ ,  $k_w = 1 \times 10^{-7} \text{ m/s}$ , n = 1.25 and  $s_a = 100 \text{ kPa}$ . The horizon is set to  $3.05\Delta x$ . The initial matric suction in the sample s = 100 kPa, (i.e.,  $S_r = 0.73$ ) and the initial isotropic stress state  $p'_0 = -73 \text{ kPa}$ .

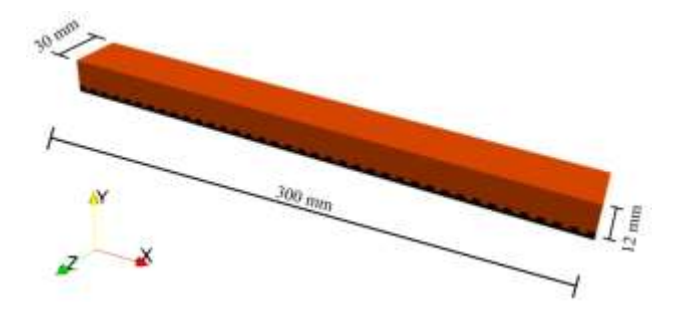


Figure 5. The problem setup for the linearly restrained desiccation test for a clay specimen.

The base of the mold is fixed while the sides are free to deform. Desiccation process is modeled as evaporation by applying a uniform external flux density on the upper surface of the clay specimen. The simulation time t = 6 hours (hr) and the time increment  $\Delta t = 1$  s.

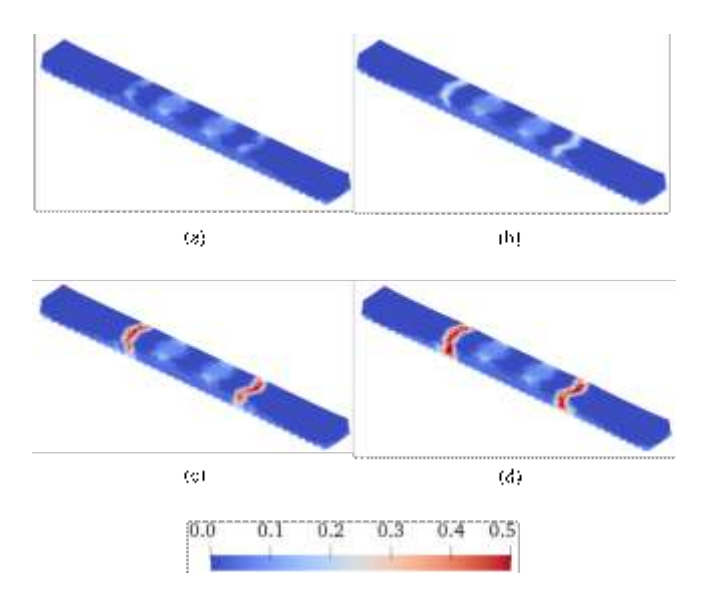


Figure 6. Contours of damage variable superimposed on deformed configuration at (a) t = 1 hr (b) t = 2 hr (c) t = 3.5 hr and (d) t = 5.5 hr.

Figures 6 and 7 plot the evolution of the crack at different stages of the simulation from an isometric and top-down view respectively. It is apparent from Figure 6 that the cracks opened at the upper surface and then propagated downward with increasing suction. Further, Figure 7 shows that the cracks occurred at the outer surface first and then propagated inward towards the longitudinal axis. This simple example has demonstrated that the proposed framework is robust in modeling desiccation cracking in clay. More numerical simulations are necessary to further evaluate the efficacy of the proposed nonlocal framework for modeling cracks in geomaterials at multiple scales.

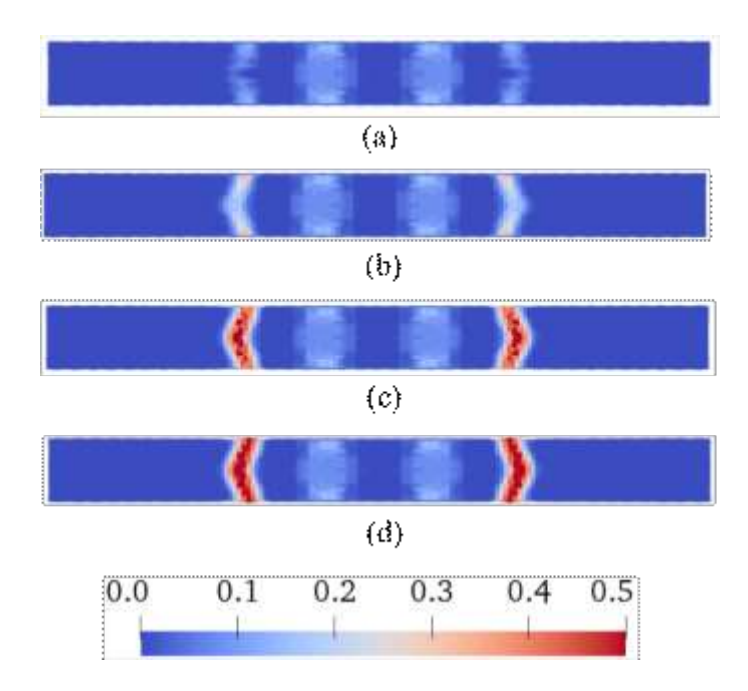


Figure 7. Top view of crack evolution (a) t = 1 hr (b) t = 2 hr (c) t = 3.5 hr and (d) t = 5.5 hr.

## **SUMMARY**

In this article, we have presented a fully coupled, three-dimensional nonlocal theory of unsaturated poromechanics for discontinuous flow-deformation analysis capable of modeling autonomous and unguided cracking. The formulation is applied to the classical problem of opening of an oblique crack and the desiccation test of a linearly restrained clay bar. The presented numerical results show that the formulation can reproduce experimentally observed trends in crack propagation. The oblique crack propagates perpendicular to the loading direction, which has been observed in laboratory experiments. For the desiccation test, the soil bar cracks open at the top and outer surface, propagating downward. The preliminary numerical results have shown that the proposed computational nonlocal unsaturated poromechanics model is robust in modeling arbitrary cracking in unsaturated soils.

# **ACKNOWLEDGEMENTS**

The work presented in this article has been supported by the US National Science Foundation under contract numbers 1659932 and 1944009.

#### REFERENCES

- Armero, F., and Simo, J. C. (1992). "A new unconditionally stable fractional step method for nonlinear coupled thermomechanical problems." *Int J Numer Methods Eng*, 35(4), 737-766.
- Fredlund, D. G., and Rahardjo, H. (1993). *Soil mechanics for unsaturated soils*. John Wiley and Sons.
- Lewis, R. W., and Schrefler, B. A. (1998). *The finite element method in the static and dynamic deformation and consolidation of porous media*. John Wiley and Sons.
- Lu, N., and Likos, W. J. (2004). Unsaturated soil mechanics. Wiley.
- Menon, S., and Song, X. (2019). "Coupled analysis of desiccation cracking in unsaturated soils through a non-local mathematical formulation." *Geosciences*, 9(10), 428.
- Menon, S., and Song, X. (2020). "Shear banding in unsaturated geomaterials through a strong nonlocal hydromechanical model." *Eur J Environ and Civ*, 1-15.
- Menon, S., and Song, X. (2021a). "A computational periporomechanics model for localized failure in unsaturated porous media." *Comput Methods Appl Mech Eng*, 359, 112770.
- Menon, S., and Song, X. (2021b). "A stabilized computational nonlocal poromechanics model for dynamic analysis of saturated porous media." *Int J Numer Meth Eng.*
- Péron, H., Delenne, J. Y., Laloui, L., and El Youssoufi, M. S. (2009). "Discrete element modelling of drying shrinkage and cracking of soils". *Comput Geotech*, 36(1-2), 61-69.
- Song, X., and Menon, S. (2019). "Modeling of chemo-hydromechanical behavior of unsaturated porous media: a nonlocal approach based on integral equations". *Acta Geotech*, 14(3), 727-747.
- Song, X., and Khalili, N. (2019). "A peridynamics model for strain localization analysis of geomaterials". *Int J Numer Anal Methods Geomech*, 43(1), 77-96.
- Song, X., and Silling, S. A. (2020). "On the peridynamic effective force state and multiphase constitutive correspondence principle." *J Mech Phys Solids*, 145, 104161.
- Zienkiewicz, O. C., Chan, A. H. C., Pastor, M., Schrefler, B. A., and Shiomi, T. (1999). *Computational geomechanics*. Chichester: Wiley.